Pten null prostate tumorigenesis and AKT activation are blocked by targeted knockout of ER chaperone GRP78/BiP in prostate epithelium

Yong Fu[a], Shiuan Wey[a], Miao Wang[a], Risheng Ye[a], Chun-Peng Liao[b], Pradip Roy-Burman[b], and Amy S. Lee[a,1]

Departments of [a]Biochemistry and Molecular Biology and [b]Pathology, University of Southern California Keck School of Medicine, University of Southern California/Norris Comprehensive Cancer Center, 1441 Eastlake Avenue, Los Angeles, CA 90089-9176

Edited by Peter K. Vogt, The Scripps Research Institute, La Jolla, CA, and approved October 17, 2008 (received for review August 8, 2008)

GRP78/BiP has recently emerged as a novel biomarker for aggressive prostate cancer. Here, we report that homozygous deletion of *Grp78* specifically in mouse prostate epithelium suppresses prostate tumorigenesis without affecting postnatal prostate development and growth. Mouse prostates with double conditional knockout of *Grp78* and *Pten* exhibit normal histology and cytology, in contrast to the invasive adenocarcinoma in mouse prostates with *Pten* inactivation. AKT activation in *Pten* null prostate epithelium is inhibited by *Grp78* homozygous deletion, corresponding with suppression of AKT phosphorylation by GRP78 knockdown in prostate cancer cell line. Thus, inactivation of GRP78 may represent a previously undescribed approach to stop prostate cancer and potentially other cancers resulting from the loss of PTEN tumor suppression and/or activation of the oncogenic AKT.

cancer suppressor | chaperone gene | inactivation

Prostate cancer is the most common cancer in men and develops through successive stages including prostatic intraepithelial neoplasia (PIN), carcinoma in situ, invasive adenocarcinoma, and metastatic disease. Although local surgery, radiation, or hormonal ablation provide initial response at early stages of the disease, tumor cells often develop resistance and relapse. Thus, the identification of new therapeutic targets for prostate cancer is of critical importance. The 78-kDa glucose regulated protein (GRP78) was initially linked to prostate cancer progression and metastasis through epitope mapping of humoral immune response from cancer patients, and identified as a functional molecular target for circulating ligands (1). Recent studies further revealed that ≈2/3 of human prostate cancers expressed high level of GRP78, associating with recurrence, development of castration-resistance, and poor survival (2, 3). These studies provide the first hints that GRP78 may have a critical role in prostate cancer development and therapeutic resistance.

GRP78, also referred to as BiP or HSPA5, is a member of the HSP70 protein family. As a major endoplasmic reticulum (ER) chaperone, GRP78 facilitates protein folding and assembly, protein quality control, ER-associated protein degradation, Ca^{2+} binding, and regulation of transmembrane ER stress inducers (4, 5). GRP78 is encoded by a single copy gene in rodents and humans. It is expressed as early as at the 2-cell stage of embryonic development, and is essential for proliferation and survival of embryonic cells (6). GRP78 is highly induced in a wide range of tumors through intrinsic factors such as altered glucose metabolism of cancer cells, compounded by extrinsic factors such as glucose deprivation, hypoxia, and acidosis in the microenvironment of poorly-perfused solid tumor (7). In a wide variety of cancer cell lines and xenograft models, GRP78 has emerged as having a critical role in cancer cell survival, tumor progression, and resistance to therapy (7–10). Despite these advances, it remains unknown whether GRP78 could also be essential for the genesis of tumor. If so, what is the underlying mechanism?

One of the most common genes involved in prostate cancer is *Pten*, a nonredundant phosphatase gene frequently deleted or mutated in human cancers (11). Loss of phosphatase and tensin homolog (PTEN) function in human cancer cell lines and mouse models results in constitutive activation of the PI3K/AKT pathway. As a result, phosphorylation of a wide range of downstream signaling molecules leads to enhanced cell growth and survival (12). *Pten* homozygous deletion in mice causes early embryonic death, and $Pten^{+/-}$ mice exhibit hyperplastic-dysplastic changes in multiple organs, including PIN in mouse prostate but no progression to adenocarcinoma (13). Conditional homozygous deletion of *Pten* in mouse prostate significantly shortens the latency of PINs and promotes their progression to metastatic cancer characteristic of human prostate cancer. The similarities between the molecular mechanisms underlying the *Pten* conditional knockout model of mouse prostate cancer and human prostate cancers are further highlighted by similar changes in the gene expression profile and the increase in focal neuroendocrine differentiation in the advanced disease in this model (14, 15).

In this study, the role of GRP78 in prostate tumorigenesis is examined in the conditional *Pten* knockout mice. Here, we describe a novel mouse model, in which both *Pten* and *Grp78* undergo biallelic inactivation specifically in the postnatal mouse prostate epithelium. This inactivation is achieved by the use of *Cre-loxP* site-specific recombination mechanism. In this system, both the alleles of each of *Pten* and *Grp78* genes are floxed out by tissue-specific Cre expression to generate the homozygous knockout. The expression of Cre recombinase is driven by PB-Cre4 promoter construct (16), which is an engineered derivative of rat probasin promoter. PB-Cre4 expression is postnatal, androgen regulated, and highly specific for prostate epithelial secretory cells, with robust activity to act on at least up to 4 alleles in a single cell (14). We discovered that specific knockout of *Grp78* in the postnatal prostate epithelium, although having no detectable effect on the development of the prostate gland, potently suppresses AKT activation and prostate tumorigenesis initiated by *Pten* homozygous deletion. Thus, inactivation of GRP78 may represent a previously undescribed approach to stop prostate cancer and other cancers resulting from the loss of PTEN tumor suppression or activation of the oncogenic AKT. The potential underlying mechanisms and clinical implications are discussed.

Author contributions: Y.F., S.W., P.R.-B., and A.S.L. designed research; Y.F. and S.W. performed research; M.W., R.Y., and C.-P.L. contributed new reagents/analytic tools; Y.F., S.W., C.-P.L., P.R.-B., and A.S.L. analyzed data; and Y.F., P.R.-B., and A.S.L. wrote the paper.

The authors declare no conflict of interest.

This article is a PNAS Direct Submission.

[1]To whom correspondence should be addressed. E-mail: amylee@ccnt.usc.edu.

This article contains supporting information online at www.pnas.org/cgi/content/full/0807691105/DCSupplemental.

www.pnas.org/cgi/doi/10.1073/pnas.0807691105

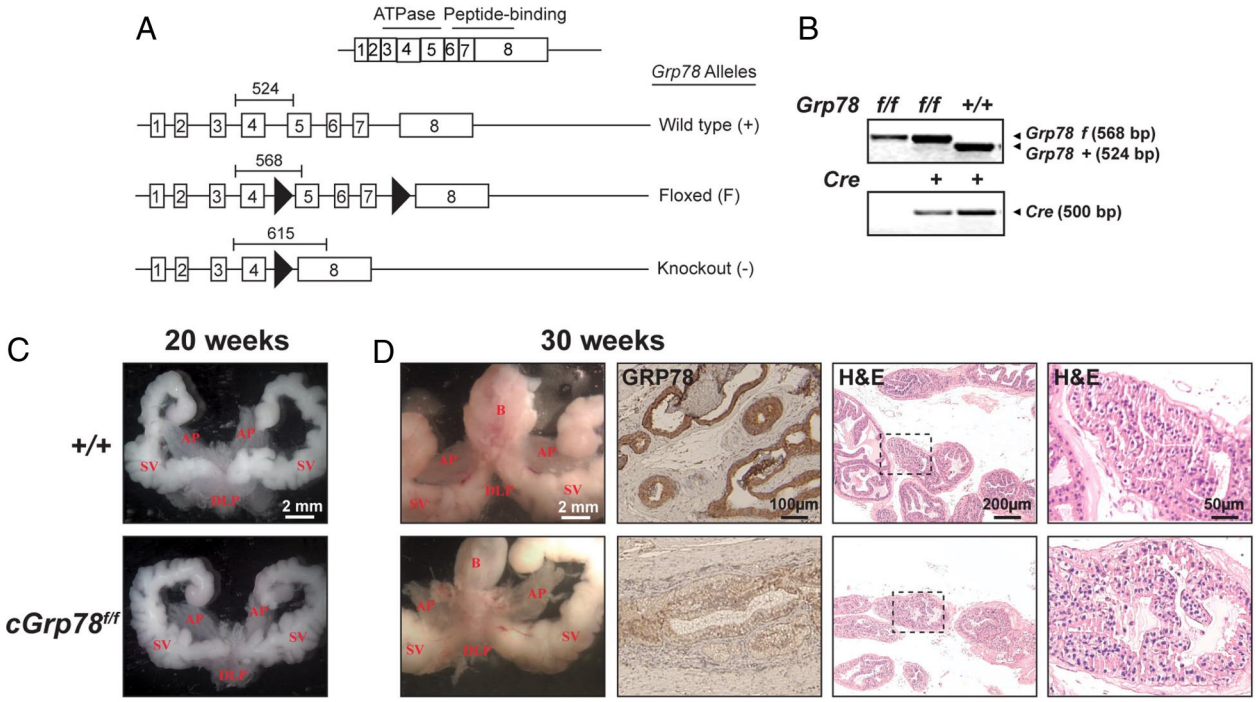

Fig. 1. Homozygous deletion of *Grp78* does not affect prostate development. (*A*) Schematic representations for the *Grp78* cDNA, the wild type allele (+), the *f* allele, and the knockout allele (−). The exons encoding the ATPase domain and peptide-binding domain of GRP78 and the loxP sites (arrow head) are indicated. The position and length of the PCR product for each allele are indicated. (*B*) PCR analysis of tail DNA from $Grp78^{f/f}$, $cGrp78^{f/f}$ and $cGrp78^{+/+}$ mice. (*C*) The gross anatomy of the prostate of $Grp78^{+/+}$ and $cGrp78^{f/f}$ mice at 20 wk. AP, anterior prostate; DLP, dorsolateral prostate; B, bladder; SV, seminal vesicle. (*D*) From left to right, images of the gross anatomy of the prostate of $Grp78^{+/+}$ and $cGrp78^{f/f}$ mice at 30 wk; immunohistochemical staining of GRP78 (depicted in brown) of DLP section, H&E staining of the DLP sections in different magnifications.

Results

Homozygous Deletion of *Grp78* Does Not Affect the Development of Prostate. Mouse *Grp78* consists of 8 exons, and the critical ATPase and peptide binding domains are contained within exons 3–5 and exons 6–8, respectively (Fig. 1*A*). In the *Grp78* floxed (*f*) allele, exons 5 through 7 are flanked by floxed sites. Previously, it was established that the knockout (−) allele generated by Cre-recombination did not produce any truncated protein (6). In this study, PB-Cre4 (abbreviated as *c*) was used to create conditional knockout in the mouse prostate epithelial cells. The scheme for the generation of the various genotypes is summarized in supporting information (SI) Fig. S1, and the genotypes were confirmed by PCR (Figs. 1*B* and 2*A*). Because GRP78 has a critical role in early embryogenesis, it is necessary to first determine whether homozygous deletion of *Grp78* in the mouse epithelium affects prostate development and growth. We observed that *PB-Cre4;*$Grp78^{f/f}$ ($cGrp78^{f/f}$) mice are phenotypically normal and fertile (data not shown). Examination at the age of 20 week (wk) revealed no difference in gross anatomy among wild type (+/+), $Grp78^{f/f}$ and $cGrp78^{f/f}$ mouse prostates, which were similar in size, morphology, the number of ductal tips, and the diameter of ducts (Fig. 1*C* and data not shown). At 30 wk, the gross anatomy of the $cGrp78^{f/f}$ mouse prostate remained normal, and immunohistochemical analysis revealed that GRP78 protein level in the prostate epithelial cells of $cGrp78^{f/f}$ mice was much lower than that of +/+ mice (Fig. 1*D*). Microscopic histology confirmed no abnormality for the $cGrp78^{f/f}$ mouse prostate, such that similar to the +/+ mice, the acini were variably sized with various amounts of epithelial infolding, all lobes had simple columnar epithelium with basophilic granular cytoplasm and centrally placed nuclei, the stroma was thin, and there was no inflammatory cell infiltration (Fig. 1*D*). Collectively, these results indicated that postnatal homozygous deletion of *Grp78* driven by PB-Cre4 affects neither the development and growth of the prostate, nor the fertility of the mouse.

Prostate Specific Homozygous Deletion of *Grp78* Blocks Prostate Tumorigenesis. To determine the role of GRP78 in prostate cancer, the $Grp78^{f/f}$ or $Grp78^{f/-}$ mice were crossed with $cPten^{f/f}$ mice. The status of *Pten* and *Grp78* deletion was determined by PCR (Fig. 2*A*). Mice of 5 distinct genotypes were used in the studies below: $Pten^{f/f}Grp78^{f/f}$; $cPten^{f/f}Grp78^{+/+}$; $cPten^{f/f}Grp78^{f/+}$; $cPten^{f/f}Grp78^{f/f}$; and $cPten^{f/f}Grp78^{f/-}$.

Between 12 to 20 wk, all $cPten^{f/f}Grp78^{+/+}$ mice (12/12) with only PTEN inactivation developed tumors in the prostate as expected. All lobes, namely anterior prostate (AP), dorsolateral prostate (DLP), and ventral prostate (VP), had solid masses and completely lost the clear fern-like appearance of prostate, compared with the $Pten^{f/f}Grp78^{f/f}$ mice (Fig. 2*B*). The 100% penetrance at 20 wk is consistent with a previous study that established the prostate specific *Pten* knockout model (15). Histological analysis, with representative images shown in Fig. 2*C* and summarized graphically in Fig. 2*D*, indicated that all $cPten^{f/f}Grp78^{+/+}$ mice developed invasive adenocarcinoma in all prostate lobes. The cancer cells exhibited nuclear enlargement and nuclear contour irregularity, as demonstrated previously (15). The malignant cells invaded through the basement membrane into the adjacent stroma, inducing both an inflammatory and a desmoplastic response, resulting in growth of fibrous and connective tissue around the tumor. In most areas, the invasion was extensive so that the glandular structure was completely lost and left with only traces of the basement membrane (Fig. 2*C*).

Strikingly, despite PTEN inactivation, none of the mice (0/8) with inactivation of both *Grp78* alleles harbored any detectable cancerous or even precancerous lesions in any of the 3 lobes of the prostate (Fig. 2 *C* and *D*). The difference in the rate of

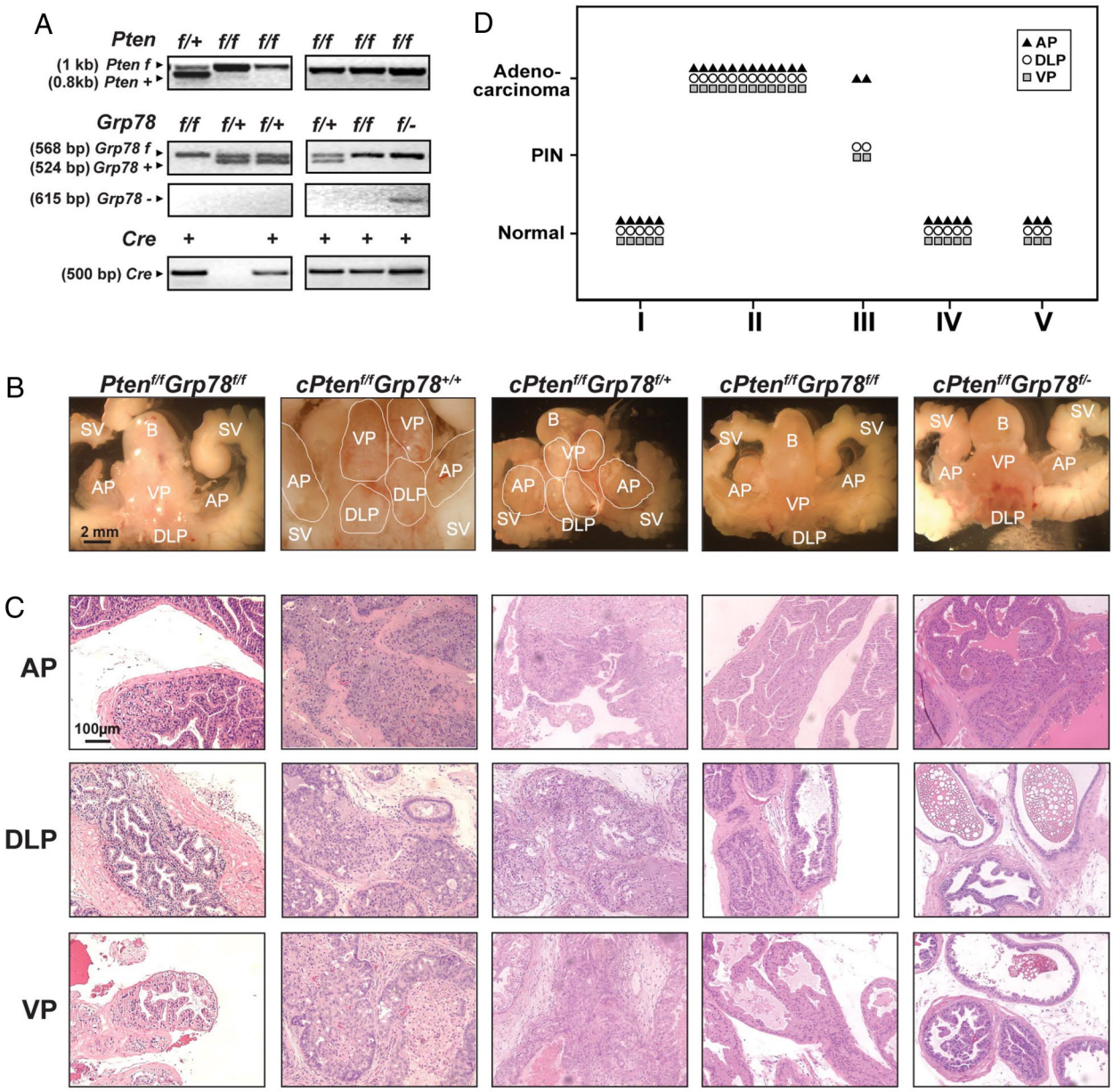

Fig. 2. Prostate specific homozygous deletion of *Grp78* blocks prostate tumorigenesis resulting from PTEN inactivation. (*A*) The *cPten*$^{f/f}$*Grp78*$^{f/+}$, *cPten*$^{f/f}$*Grp78*$^{f/f}$, and *cPten*$^{f/f}$*Grp78*$^{f/-}$ male mice were genotyped by PCR analysis. (*B*) The gross anatomy of the prostate of the mice with the indicated genotypes at 20 wk. All lobes of *cPten*$^{f/f}$*Grp78*$^{+/+}$ mice formed solid tumor mass. In *cPten*$^{f/f}$*Grp78*$^{f/+}$ mice, only AP developed solid tumor mass. The *cPten*$^{f/f}$*Grp78*$^{f/f}$ and *cPten*$^{f/f}$*Grp78*$^{f/-}$ mice are normal and cancer free. AP, anterior prostate; DLP, dorsolateral prostate; VP, ventral prostate; B, bladder; SV, seminal vesicle. (*C*) Histological comparison of H&E staining prostate sections of the mice in *B*. The *cPten*$^{f/f}$*Grp78*$^{+/+}$ mice developed invasive adenocarcinoma in all prostate lobes. In *cPten*$^{f/f}$*Grp78*$^{f/+}$ mice, AP had extensive invasive adenocarcinoma, whereas DLP and VP only developed diffusive prostate intraepithelial neoplasia (PIN). All lobes of the *cPten*$^{f/f}$*Grp78*$^{f/f}$, and *cPten*$^{f/f}$*Grp78*$^{f/-}$ mouse prostates were normal. (*D*) The distribution of prostate lobes in 3 histological states, normal, PIN, and adenocarcinoma, for each genotype: *Pten*$^{f/f}$*Grp78*$^{f/f}$ (I), *cPten*$^{f/f}$*Grp78*$^{+/+}$ (II), *cPten*$^{f/f}$*Grp78*$^{f/+}$ (III), *cPten*$^{f/f}$*Grp78*$^{f/f}$ (IV), and *cPten*$^{f/f}$*Grp78*$^{f/-}$ (V).

prostate cancer between *Pten* null mice (12/12) and *Pten*/*Grp78* double conditional knockout mice (0/8) is statistically significant by Fisher's exact test with 2-sided $P < 0.0001$. At necropsy at the age of 20 wk, for both *cPten*$^{f/f}$*Grp78*$^{f/f}$ mice ($n = 5$) and the *cPten*$^{f/f}$*Grp78*$^{f/-}$ mice ($n = 3$), the gross fern-like prostate morphology had clear and gelatinous ducts. The number of ductal tips and the diameter of ducts did not show any obvious difference, compared with the *Pten*$^{f/f}$*Grp78*$^{f/f}$ mice (Fig. 2*B*). Also, the microanatomy of the prostate appeared generally normal, including the density of epithelial cells, their morphology, and the size and organization of the gland (Fig. 2*C*). There was only mild to moderate hyperplasia in occasional areas, with normal cytological features and intact basement membrane, which was also observed in age-matched wild type mice as reported previously (17). Correspondingly, the *cPten*$^{f/f}$*Grp78*$^{f/+}$ mice ($n = 2$) where *Grp78* is heterozygous exhibited an intermediate phenotype (Fig. 2 *B–D*); whereas AP developed grossly visible solid tumor mass with invasive adenocarcinoma, the DLP and VP lobes still kept the fern-like ductal structure albeit with enlarged ducts. Correspondingly, the microanatomy of DLP and VP only exhibited diffusive PIN with the intact basement membrane (Fig. 2*C*). These observations are consistent with PB-CRE4 being more effective in the DLP and VP than AP in young mice (15).

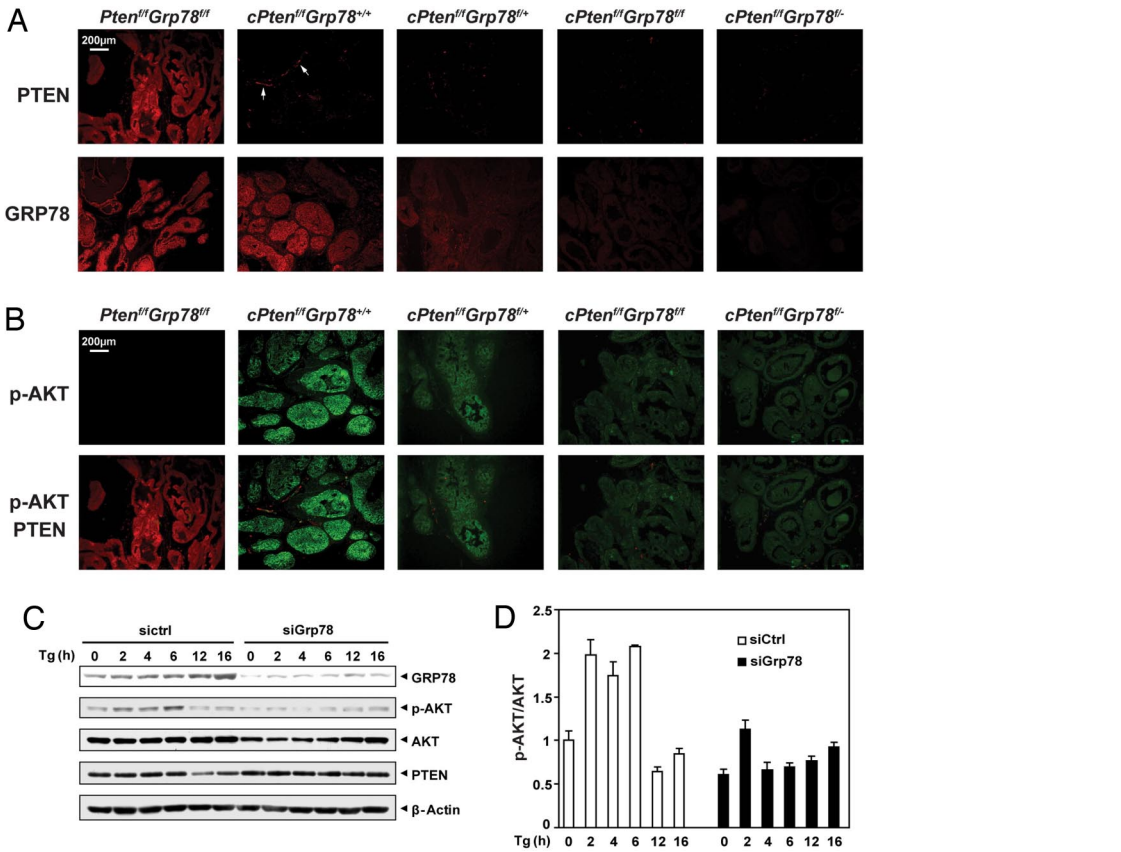

Fig. 3. Knockout of GRP78 Inhibits the AKT activation. (*A*) Immunofluorescence staining of PTEN and GRP78 in the DLP of mice with the indicated genotypes. The stromal cells in mutant prostates remained PTEN positive (white arrow), which confirmed the *PB-Cre4* mediated deletion is prostate epithelium specific. (*B*) Immunofluorescence staining of p-AKT (Ser-473) and the double staining of p-AKT and PTEN of prostate sections of the mice in *A*. Staining for p-AKT was strong in the prostate epithelium of $cPten^{f/f}Grp78^{+/+}$ mice, decreased in the $cPten^{f/f}Grp78^{f/+}$ mice, and further decreased in the $cPten^{f/f}Grp78^{f/f}$ and $cPten^{f/f}Grp78^{f/-}$ mice. (*C*) GRP78 knockdown inhibits AKT phosphorylation. Human prostate cancer cell line PC3 was transfected with siRNA against GRP78 (siGrp78) or control siRNA (siCtrl), and then treated with 300-nM Tg. Cells were harvested at the time points (in hours) as indicated and subjected to Western blotting. (*D*) The ratio of p-AKT to total AKT level in *C* was quantitated. The ratio at the 0 h time point in cells transfected with siCtrl was set as 1.

To confirm the expression level of PTEN and GRP78 in the mouse prostates of the 5 genotypes, immunofluorescence staining was performed. Representative images for the DLP, which exhibits most similarity to the peripheral zone of the human prostate where most of the cancers occur, are shown in Fig. 3*A*; images for AP and VP are shown in Fig. S2*A* and Fig. S3*A*. PTEN immunofluorescence staining was clearly visible in the $Pten^{f/f}Grp78^{f/f}$ mice but were greatly reduced in the prostate of all mice where *Pten* was inactivated ($cPten^{f/f}Grp78^{+/+}$, $cPten^{f/f}Grp78^{f/+}$, $cPten^{f/f}Grp78^{f/f}$, and $cPten^{f/f}Grp78^{f/-}$). GRP78 immunofluorescence staining was detected in the prostate of the $Pten^{f/f}Grp78^{f/f}$ and $cPten^{f/f}Grp78^{+/+}$ mice, reduced in the heterozygous $cPten^{f/f}Grp78^{f/+}$ mice, and nearly undetectable in the $cPten^{f/f}Grp78^{f/f}$, and $cPten^{f/f}Grp78^{f/-}$ mice where *Grp78* was inactivated. Thus, the PTEN and GRP78 expression levels correspond with the respective genotypes and loss of GRP78 potently suppresses prostate tumorigenesis resulting from the loss of PTEN.

Loss of GRP78 Inhibits Activation of the Oncogenic Kinase AKT. To understand how GRP78 blocks prostate tumor initiation, we examined the phosphorylation of AKT, which is the primary target of the PTEN signaling pathway (15). Phosphorylated AKT (p-AKT) was detected by the immunofluorescence staining by using anti-p-AKT antibody against serine 473. Representative images for the DLP are shown in Fig. 3*B*; images for AP and VP are shown in Fig. S2*B* and Fig. S3*B*. In all 3 lobes, no p-AKT immunofluorescence staining was detected in the prostate of the Cre-negative $Pten^{f/f}Grp78^{f/f}$ mice. In contrast, strong p-AKT staining was observed in the $cPten^{f/f}Grp78^{+/+}$ mouse prostate where *Pten* was inactivated. The positive AKT staining was primarily in the epithelium with only a scattered and a very low level of staining in the stroma with positive PTEN staining, consistent with the scenario that AKT phosphorylation was caused by PTEN nullification. In parallel with the reduction in GRP78 level and inhibition of tumorigenesis, p-AKT level was diminished in the histological sections (Fig. 3*B*). Quantitation of p-AKT immunofluorescence indicates that the p-AKT level was reduced significantly: by 45% in the heterozygous $cPten^{f/f}Grp78^{f/+}$ mouse prostate, and by 75% in the prostate of the double conditional knockout $cPten^{f/f}Grp78^{f/f}$ and $cPten^{f/f}Grp78^{f/-}$ mice (Fig. S4).

The tumor microenvironment is subject to ER stress, which may modulate AKT activation. To determine whether GRP78 is required for AKT phosphorylation in prostate cancer cells, we used siRNA to specifically knockdown GRP78 expression and examined its effect on p-AKT phosphorylation at serine 473. In prostate cancer PC-3 cells transfected with control siRNA, treatment with thapsigargin (Tg), an ER stress inducer, increased GRP78 level gradually as expected. The level of p-AKT was increased by short exposure to Tg (peak at 6 h), but decreased on longer exposure (12 to 16 h), whereas the total AKT level remained unchanged (Fig. 3*C*). Similar observations have been reported for glial and breast cancer cells (18, 19). In

cells transfected with siRNA against GRP78, AKT phosphorylation in Tg-treated cells was inhibited by GRP78 knockdown (Fig. 3*C*). The ratio of p-AKT to total AKT level under each experimental condition is summarized in Fig. 3*D*. Thus, in parallel to the suppression of p-AKT staining in the prostate of mouse models where both *Grp78* and *Pten* are inactivated, AKT activation could also be suppressed by knockdown of GRP78 in prostate cancer cells.

Discussion

In this study, we demonstrate that specific elimination of a single molecular entity, GRP78, from the mouse prostate epithelial cells can suppress AKT activation and block prostate cancer development initiated by the loss of PTEN, which is a powerful tumor suppressor gene for a wide variety of human cancers. While by 3 to 4 months of age the incidence of spontaneous prostate cancer is 100% in the conditional biallelic *Pten* deletion model, simultaneous homozygous inactivation of *Grp78* in the prostate epithelium potently suppresses tumor formation, because no traces of cancer could be detected even after >4 months of observation. It is unlikely that the suppression of tumor formation is due to strain background variation, because $cPten^{f/f}Grp78^{f/+}$ mice developed adenocarcinoma at 20 wk, whereas the $cPten^{f/f}Grp78^{f/f}$ littermates with similar mixed genetic background were free of cancer. Also, double conditional knockout $cPten^{f/f}Grp78^{f/f}$ mouse at 40 wk only developed PIN (Y.F. and A.S.L., unpublished results), in contrast to the metastasis or death in $cPten^{f/f}$ mice from 12 to 29 wk observed by us and others (15). Supporting the result of the mouse model study, knockdown of GRP78 by siRNA in human prostate cancer cells inhibited AKT phosphorylation, which is consistent with previous reports that GRP78 down-regulation inhibited AKT activation in 1-LN prostate cancer cells with intact PTEN (20) and in human endothelial cells (21). Thus, our studies suggest a mechanistic explanation, by which a prominent effector, namely AKT that is activated by loss of PTEN, is severely compromised by the absence of GRP78 function in prostate epithelial cells.

In contrast to our observations, knockout of systemic IGF1 or prostatic IGF1R, both of which are an upstream factor of AKT, does not affect carcinogenesis in the prostate (22, 23). This observation suggests that the effect of GRP78 on AKT activation is specific. How might GRP78 influence AKT activity and confer growth and survival advantage to precancerous cells? Two major mechanisms may be involved: the ability of GRP78 to enhance cell proliferation and protect against stress associated with tumorigenesis (7). With regard to proliferation, as a major ER chaperone, GRP78 may facilitate the processing and trafficking of critical growth factors and their receptors to the cell surface. Also, GRP78 can exist as a cell surface protein in some cell types, including prostate cancer cells and transmit extracellular stimuli to intracellular AKT signaling pathways to promote both growth and survival (20, 21, 24). In addition to maintenance of ER homeostasis through protein quality control and serving as an ER Ca^{2+} binding protein, GRP78 with antiapoptotic properties is known to protect cancer cells against immune surveillance (25), and directly interacts with and inhibits caspase-7 (26). Also, GRP78 could block initiation of apoptosis by inhibiting the proapoptotic BH3 protein BIK, which is a downstream effector of p53 and its loss is implicated in the development of human breast and colorectal cancers (9, 27). Recently, it was reported that PTEN deficiency enhances hypoxia-induced ER stress including the up-regulation of GRP78 (28), suggesting that GRP78 may be required for survival of PTEN null cells under stress conditions during tumorigenesis. Most recently, GRP78 is determined to be obligatory for stress-induced autophagy, which has been implicated in cancer progression (29). It is also tempting to speculate that GRP78 may have a role in cancer stem cells, because it is required for survival of embryonic stem cell precursors and is among a set of select genes expressed in hematopoietic stem cells (6, 30). Thus, although loss of PTEN provides strong initiating force for tumor development, the failure to fully activate the AKT pathway along with the increase in apoptosis resulting from the loss of GRP78 may potently suppress the oncogenic steps after initiation through potentially selective elimination of precancerous cells. The details of the mechanism of GRP78 regulation of AKT activation await further investigations.

Also, despite the known embryonic lethality of conventional knockout of *Grp78* (6), we further established that the development and growth of the prostate gland are not hindered by the PB-Cre4 mediated conditional knockout of GRP78 function in the prostate epithelium. In a transgenic mouse model of mammary tumor, *Grp78* heterozygosity does not affect organ development and growth, but prolongs the tumor latency period, increases apoptosis, suppresses tumor proliferation, and specifically blocks tumor angiogenesis (31). This finding implies GRP78 facilitates blood vessel formation required for oncogenic progression, although it remains to be determined whether this effect is due to host or tumor factors. The same study also provides the proof-of-principle that drugs that partially suppress GRP78 expression and/or activity will have minimal impact on major organ function, but preferably halt cancer progression. With the recent identification of agents that block GRP78 expression or activity, anti-GRP78 therapy, in combination with conventional therapy, may open up a novel approach to stop human cancer (7).

Materials and Methods

Generation of the Prostate-Specific *Pten* and *Grp78* Homozygous Deletion Mice. *Grp78 T*/+ mice carrying the targeted allele (*T*) (6) were mated with EIIA-cre transgenic mice and generated offspring carrying the *f* or knockout (−) allele on C57BL/6 background. The parental male mouse harboring the *PB-Cre4* transgene and *f Pten* allele on C57BL/6xDBA2/129 background was described previously (15). The breeding scheme of the various mouse genotypes is described in Fig. S1.

Immunohistochemistry Analysis. The paraffin sections were first deparaffinized and rehydrated, and antigens were retrieved by means of incubation of slides in Retrievagen A Solution (BD PharMingen) at 95–100 °C for 30 min. Slides were then allowed to cool at room temperature for 1 h in Retrievagen A Solution. After washing with double distilled water and PBS, the slides were washed twice in 3% H_2O_2 in PBS for 5 min to eliminate endogenous peroxidase activity. The slides were subsequently blocked; for monoclonal primary antibodies, sections were blocked with the horse serum (ABC Elite kit, Vector Laboratories); for polyclonal primary antibodies, sections were blocked with the goat serum of ABC Elite kit. After blocking, sections were incubated overnight with polyclonal rabbit anti-GRP78 (H-129, Santa Cruz Biotechnology) diluted at 1:200 in blocking solution (ABC Elite Kit, Vector Laboratories) at 4 °C. After three 5-min washings in PBS, sections were then incubated with biotinylated anti-rabbit secondary antibody (ABC Elite Kit, Vector Laboratories) for 30 min at room temperature. After PBS washings, sections were developed with the ABC Elite kit according to manufacturer's protocol. Slides were then counterstained with hematoxylin, dehydrated, and cover slipped. Negative control slides were processed without primary antibody.

Immunofluorescence Analysis. The paraffin sections were first deparaffinized and rehydrated, and antigens were retrieved by means of incubation of slides in Retrievagen A Solution (BD PharMingen) at 95–100 °C for 30 min. Slides were then allowed to cool at room temperature for 1 h in Retrievagen A Solution. After washing in double distilled water and PBS, the slides were blocked with 1% BSA in PBS for 30 min at room temperature. After removing excessive blocking solution, sections were incubated with primary antibodies at 4 °C overnight. After three 5-min washings in PBS, sections were then incubated with FITC-conjugated anti-mouse or rhodamine-conjugated anti-rabbit antibody for 60 min at room temperature. Slides were then dehydrated and coverslipped. Negative control slides were processed without primary antibody. Primary antibodies were polyclonal rabbit anti-PTEN (26H9, no.

9556; Cell Signaling Technology), monoclonal mouse anti-p-AKT (Ser-473, no. 9271S; Cell Signaling Technology), monoclonal mouse anti-GRP78 (no. 610978; BD PharMingen). All primary antibodies were diluted at 1:200 in 1% BSA in PBS. The immunofluorescence was quantitated by using the NIH software ImageJ (version 1.40g).

Details on autopsy and histopathology assessments, genotyping of mice, cell culture and treatment, and Western blottings are described in *SI Materials and Methods*.

ACKNOWLEDGMENTS. We thank Dr. Hong Wu (University of California, Los Angeles) for generously providing the *f*PTEN mouse strain; Drs. Louis Dubeau, Hooman Allayee, Gerhard Coetzee, Martin Kast, Omar Khalid, and Andrew Gray for helpful discussion and assistance; and the University of Southern California/Norris Comprehensive Cancer Center Translational Pathology Core Facility for preparation of histological sections. This work was supported in part by National Cancer Institute Grants CA27607 (to A.S.L.) and CA113392 (to P.R.-B.).

1. Mintz PJ, *et al.* (2003) Fingerprinting the circulating repertoire of antibodies from cancer patients. *Nat Biotechnol* 21:57–63.
2. Daneshmand S, *et al.* (2007) Glucose-regulated protein GRP78 is up-regulated in prostate cancer and correlates with recurrence and survival. *Hum Pathol* 38:1547–1552.
3. Pootrakul L, *et al.* (2006) Expression of stress response protein Grp78 is associated with the development of castration-resistant prostate cancer. *Clin Cancer Res* 12:5987–5993.
4. Hendershot LM (2004) The ER function BiP is a master regulator of ER function. *Mt Sinai J Med* 71:289–297.
5. Ni M, Lee AS (2007) ER chaperones in mammalian development and human diseases. *FEBS Lett* 581:3641–3651.
6. Luo S, Mao C, Lee B, Lee AS (2006) GRP78/BiP is required for cell proliferation and protecting the inner cell mass from apoptosis during early mouse embryonic development. *Mol Cell Biol* 26:5688–5697.
7. Lee AS (2007) GRP78 induction in cancer: Therapeutic and prognostic implications. *Cancer Res* 67:3496–3499.
8. Li J, Lee AS (2006) Stress induction of GRP78/BiP and its role in cancer. *Curr Mol Med* 6:45–54.
9. Fu Y, Li J, Lee AS (2007) GRP78/BiP inhibits endoplasmic reticulum BIK and protects human breast cancer cells against estrogen-starvation induced apoptosis. *Cancer Res* 67:3734–3740.
10. Pyrko P, *et al.* (2007) The unfolded protein response regulator GRP78/BiP as a novel target for increasing chemosensitivity in malignant gliomas. *Cancer Res* 67:9809–9816.
11. Salmena L, Carracedo A, Pandolfi PP (2008) Tenets of PTEN tumor suppression. *Cell* 133:403–414.
12. Sansal I, Sellers WR (2004) The biology and clinical relevance of the PTEN tumor suppressor pathway. *J Clin Oncol* 22:2954–2963.
13. Di Cristofano A, Pesce B, Cordon-Cardo C, Pandolfi PP (1998) Pten is essential for embryonic development and tumour suppression. *Nat Genet* 19:348–355.
14. Liao CP, *et al.* (2007) Mouse models of prostate adenocarcinoma with the capacity to monitor spontaneous carcinogenesis by bioluminescence or fluorescence. *Cancer Res* 67:7525–7533.
15. Wang S, *et al.* (2003) Prostate-specific deletion of the murine Pten tumor suppressor gene leads to metastatic prostate cancer. *Cancer Cell* 4:209–221.
16. Wu X, *et al.* (2001) Generation of a prostate epithelial cell-specific Cre transgenic mouse model for tissue-specific gene ablation. *Mech Dev* 101:61–69.
17. Roy-Burman P, *et al.* (2004) Genetically defined mouse models that mimic natural aspects of human prostate cancer development. *Endocr Relat Cancer* 11:225–254.
18. Hosoi T, *et al.* (2007) Akt up- and down-regulation in response to endoplasmic reticulum stress. *Brain Res* 1152:27–31.
19. Hu P, Han Z, Couvillon AD, Exton JH (2004) Critical role of endogenous Akt/IAPs and MEK1/ERK pathways in counteracting endoplasmic reticulum stress-induced cell death. *J Biol Chem* 279:49420–49429.
20. Misra UK, Deedwania R, Pizzo SV (2006) Activation and cross-talk between Akt, NF-{kappa}B, and unfolded protein response signaling in 1-LN prostate cancer cells consequent to ligation of cell surface-associated GRP78. *J Biol Chem* 281:13694–13707.
21. Philippova M, *et al.* (2008) Identification of proteins associating with glycosylphosphatidylinositol- anchored T-cadherin on the surface of vascular endothelial cells: Role for Grp78/BiP in T-cadherin-dependent cell survival. *Mol Cell Biol* 28:4004–4017.
22. Anzo M, *et al.* (2008) Targeted deletion of hepatic Igf1 in TRAMP mice leads to dramatic alterations in the circulating insulin-like growth factor axis but does not reduce tumor progression. *Cancer Res* 68:3342–3349.
23. Sutherland BW, *et al.* (2008) Conditional deletion of insulin-like growth factor-I receptor in prostate epithelium. *Cancer Res* 68:3495–3504.
24. Arap MA, *et al.* (2004) Cell surface expression of the stress response chaperone GRP78 enables tumor targeting by circulating ligands. *Cancer Cell* 6:275–284.
25. Sugawara S, Takeda K, Lee A, Dennert G (1993) Suppression of stress protein GRP78 induction in tumor B/C10ME eliminates resistance to cell mediated cytotoxicity. *Cancer Res* 53:6001–6005.
26. Reddy RK, *et al.* (2003) Endoplasmic reticulum chaperone protein GRP78 protects cells from apoptosis induced by topoisomerase inhibitors: Role of ATP binding site in suppression of caspase-7 activation. *J Biol Chem* 278:20915–20924.
27. Castells A, Gusella JF, Ramesh V, Rustgi AK (2000) A region of deletion on chromosome 22q13 is common to human breast and colorectal cancers. *Cancer Res* 60:2836–2839.
28. Yang G, *et al.* (2008) PTEN deficiency causes dyschondroplasia in mice by enhanced hypoxia-inducible factor 1α signaling and endoplasmic reticulum stress. *Development* 135:3587–3897.
29. Li J, *et al.* (2008) The unfolded protein response regulator GRP78/BiP is required for endoplasmic reticulum integrity and stress-induced autophagy in mammalian cells. *Cell Death Differ* 15:1460–1471.
30. Chambers SM, *et al.* (2007) Aging hematopoietic stem cells decline in function and exhibit epigenetic dysregulation. *PLoS Biol* 5:e201.
31. Dong D, *et al.* (2008) Critical role of the stress chaperone GRP78/BiP in tumor proliferation, survival and tumor angiogenesis in transgene-induced mammary tumor development. *Cancer Res* 68:498–505.